PROGRESS IN COLOR, COLORANTS AND COATINGS

available online @ www.pccc.icrc.ac.ir

Progress in Color Colorants Coating 17 (2024), 185-205

Ministry of Science, Research and Technology
Institute for Color Science & Technology

Investigating the Corrosion Inhibition Performance of Methyl 3H-2,3,5-triazole-1-formate for Mild Steel in Hydrochloric Acid Solution: Experimental and Theoretical Insights

Ali M. Resen[1], Ayad N. Jasim[2], Heba S. Qasim[1], Mahdi M. Hanoon[1], Ahmed A. Al-Amiery[3,4,*], Waleed Khalid Al-Azzawi[5], Ali M. Mustafa[1], Firas F. Sayyid[1]

[1.] Production Engineering and Metallurgy, University of Technology-Iraq, Baghdad, P.O. Box: 10001, Iraq
[2.] Materials engineering, Department, Diyala University, P.O. Box: 32001, Diyala, Iraq
[3.] Department of Chemical and Process Engineering, Faculty of Engineering and Built Environment, Universiti Kebangsaan Malaysia (UKM), P.O. Box: 43000, UKM Bangi, Selangor, Malaysia
[4.] Energy and Renewable Energies Technology Center, University of Technology-Iraq, Baghdad, P.O. Box: 10001, Iraq.
[5.] Al-Farahidi University, Baghdad, P.O. Box: 10001, Iraq

ARTICLE INFO

Article history:
Received: 21 Aug 2023
Final Revised: 21 Oct 2023
Accepted: 25 Oct 2023
Available online: 26 Dec 2023

Keywords:
Triazole
Corrosion inhibitor
Quantum chemical,
DFT

ABSTRACT

Corrosion presents a formidable challenge to the durability of metallic materials, especially in aggressive environments. This study delves into the corrosion inhibition capabilities of Methyl 3H-2,3,5-triazole-1-formate when applied to mild steel immersed in a 1 M HCl solution. Weight loss techniques meticulously scrutinize the inhibitor's efficacy across concentrations (0.1, 0.2, 0.3, 0.4, 0.5, and 1 mM). Immersion durations (1, 5, 10, 24, and 48 hours), all conducted at a constant temperature of 303 K. Furthermore, we explore the influence of temperature fluctuations (ranging from 303 to 333 K) on varying inhibitor concentrations (0.1-1 mM) through a 5-hour immersion period. To delve deeper into the molecular interactions underpinning the inhibitor's effects, we employ Density Functional Theory (DFT) calculations, harnessing the Gaussian 09 software package. Leveraging the B3LYP method, which fuses exchange and correlation functionals alongside a 6-31G++(d,p) basis set, our investigation yields critical insights. Complementary to this analysis, we determine pivotal molecular descriptors, encompassing electronegativity (χ), hardness (η), softness (σ), and transferred electrons fractional number (ΔN). Our experimental findings underscore the inhibitor's prowess, showcasing an impressive inhibition efficiency of 93.8 % at the optimized concentration of 5 mM and an immersion duration of 5 hours at 303 K. Also, we discern that the adsorption behavior of the inhibitor on the mild steel surface aligns with the Langmuir adsorption isotherm, shedding light on its interaction mechanisms. These comprehensive findings hold profound implications for advancing corrosion protection strategies and optimizing inhibitor applications across diverse industrial settings.Prog. Color Colorants Coat. 17 (2024), 185-205© Institute for Color Science and Technology.

1. Introduction

The corrosion of metallic materials remains a pervasive and persistent challenge that reverberates across diverse industrial sectors, exacting substantial economic tolls and engendering heightened safety concerns. One particular material, mild steel, extensively used in construction and manufacturing, is particularly susceptible to the insidious process of

*Corresponding author: * dr.ahmed1975@ukm.edu.my
dr.ahmed1975@gmail.com

https://doi.org/10.30509/pccc.2023.167189.1245

corrosion, especially when exposed to aggressive environments such as HCl solutions. Developing effective corrosion inhibitors has emerged as a focus of research attention to combat this predicament. These inhibitors operate by erecting a protective barrier on the surface of the metal, effectively impeding the electrochemical reactions that propel corrosion [1-4]. Among the countless compounds investigated for their corrosion inhibition ability, methyl 3H-2,3,5-triazol-1-formate has emerged as an interesting and promising candidate. Its chemical structure suggests an inherent capacity for favorable interactions with metal surfaces, potentially culminating in forming a protective layer that effectively thwarts corrosive processes [5, 6]. The choice of this compound as the subject of our investigation holds paramount significance. It deepens our fundamental understanding of corrosion inhibition mechanisms, offering opportunities to optimize its industrial application to mitigate the pernicious effects of corrosion [7].

Researchers have harnessed various techniques to assess inhibition efficiency, adsorption behavior, and molecular interactions in pursuing effective corrosion inhibitors. Among these multi-faceted approaches, weight loss techniques have gained great importance. This experimental method provides invaluable quantitative insights into the extent of corrosion inhibition under varying conditions, including different inhibitor concentrations and immersion durations. In complement to experimental investigations, theoretical methods, most notably Density Functional Theory (DFT), furnish an alternative perspective. These computational tools enable meticulous explorations of electronic structures, molecular interactions, and reactivity patterns of inhibitor molecules [8-12]. Within the expansive landscape of corrosion inhibition research, a rich tapestry of organic compounds has been scrutinized for their potential to protect mild steel in acidic environments [13, 14]. These compounds are meticulously selected based on their chemical structures, often characterized by nitrogen, oxygen, and sulfur functional groups, which facilitate their adsorption onto metal surfaces. Recent investigations have underscored the promise of triazole derivatives, primarily due to their heteroatomic compositions, promoting strong interactions with metal surfaces [15-18]. To holistically assess the efficacy of corrosion inhibitors and illuminate the intricate mechanisms underpinning their action, researchers have embraced a multi-faceted approach that integrates both experimental and computational dimensions. Experimental techniques encompass a spectrum of methods, including weight loss measurements, electrochemical impedance spectroscopy (EIS), and polarization studies. These empirical approaches provide valuable insights into the kinetics and thermodynamics of corrosion processes and inhibitors' behaviour under various conditions.

Conversely, computational methods, particularly DFT, empower researchers to delve deeply into the electronic structures and bonding characteristics of inhibitor molecules, revealing the nature of their interactions with metal surfaces [19-23]. In theoretical calculations, the B3LYP functional, a prominent hybrid functional, has exhibited a commendable track record in accurately predicting molecular properties and interactions [24-26]. DFT calculations, often coupled with diverse basis sets, have played a pivotal role in analyzing adsorption energies, electronic properties, and molecular descriptors, shedding light on inhibitors' reactivity and stability. This synergistic approach, which amalgamates theoretical insights with experimental findings, advances our comprehension of the corrosion inhibition mechanism and informs the design of novel and efficient inhibitors [27-30].

The current study is preparing to bridge the gap between these experimental and theoretical methods. Our overarching objective is to probe the corrosion inhibition properties of Methyl 3H-2,3,5-triazole-1-formate (Figure 1) concerning mild steel submerged in a 1 M HCl solution. The selection of this inhibitor is underpinned by several compelling factors, including its chemical structure, which suggests a penchant for strong interactions with metal surfaces. The choice of this inhibitor is predicated on its potential significance and the expectation that it may offer unique properties conducive to effective corrosion inhibition.

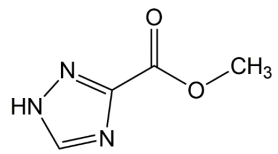

Figure 1: The chemical structure of methyl 3H-2,3,5-triazole-1-formate.

By examining the inhibitor's performance across diverse concentrations, immersion durations, and temperatures and harnessing advanced computational techniques, we aspire to unravel the intricate interactions underpinning corrosion inhibition. In doing so, we aim to make a substantive contribution to advancing corrosion protection strategies and refining inhibitor applications in industrial contexts, offering innovative solutions to the pervasive challenge of corrosion.

Studying corrosion inhibition processes in acidic environments is paramount in materials science and engineering. Acidic solutions, particularly HCl, are widely employed in industrial processes, chemical manufacturing, and various applications, rendering materials susceptible to corrosion. The rationalization behind investigating corrosion inhibition in acid solutions is multi-faceted and encompasses several key aspects [31, 32].

In the oil and gas industry, HCl is extensively used in numerous industrial processes, including pickling, metal cleaning, and acidizing. The aggressive nature of HCl can lead to substantial corrosion-related economic losses, making corrosion inhibition research imperative. Understanding the inhibitory mechanisms and effectiveness of specific compounds in acid solutions can pave the way for developing efficient and cost-effective corrosion control strategies [33, 34].

The maintenance and longevity of infrastructure components, such as pipelines, storage tanks, and chemical reactors, often rely on their ability to withstand exposure to acidic environments. Corrosion in such critical structures can compromise safety, environmental integrity, and operational efficiency. By comprehensively studying corrosion inhibition in acid solutions, we can contribute to the preservation and durability of these essential assets [35, 36].

Mitigating corrosion in acidic environments is not only necessary for economic reasons but also for environmental conservation. Corrosion-related failures can result in hazardous material leaks, environmental contamination, and regulatory violations. Effective inhibition strategies can reduce the risk of such incidents, promoting sustainability and minimizing the environmental footprint of industrial processes [37, 38].

Developing novel materials and inhibitors capable of withstanding aggressive acidic conditions is at the forefront of corrosion science and engineering. Research in this domain is vital for advancing technology and innovation, enabling the design of more resilient materials and coatings for various applications.

Studying corrosion inhibition in acid solutions provides valuable insights into the fundamental principles of surface interactions, electrochemistry, and material behavior. These insights extend beyond the specific application, fostering a deeper understanding of corrosion mechanisms in diverse environments.

In conclusion, the choice to investigate corrosion inhibition in acid solutions, particularly HCl, is motivated by its profound relevance and significance in industrial, environmental, and technological contexts. This research endeavours to contribute to developing effective corrosion control strategies, protecting critical infrastructure, and advancing materials science, with broader implications for industrial and societal well-being.

2. Experimental

2.1. Materials and reagents

The inhibitor, methyl 3H-2,3,5-triazole-1-formate, utilized in this study was procured from Sigma-Aldrich, a reputable chemical supplier in Selangor, Malaysia. Notably, the inhibitor was employed in its as-received state without undergoing additional purification processes. Mild steel specimens from a metals company with the composition percentage C = 0.21, Si = 0.38, Mn = 0.05, P = 0.09, Al = 0.01 and Fe = 99.21 were carefully prepared to ensure uniformity and consistency in the experimental setup. The mild steel samples, with dimensions of 4.5 × 1 × 0.02 cm, following ASTM G1-03 protocol [39, 40], were initially mechanically polished to a mirror-like finish using fine-grit abrasive papers. This step was crucial to eliminate any pre-existing surface irregularities that could influence the corrosion behavior. Subsequently, the specimens were thoroughly cleaned using acetone and rinsed with deionized water to remove any residual contaminants. The prepared samples were then air-dried to prevent the formation of oxide layers before the commencement of experiments. The characterization process involved surface profiling using profilometry to verify the smoothness and consistency of the prepared specimens. Mild steel specimens were used as the working electrode in this study. Methyl 3H-2,3,5-triazole-1-formate, the corrosion inhibitor of interest, was dissolved in the smallest amount of methanol. Then, we completed the volume with a 1 M hydrochloric acid solution to obtain

the required concentrations. The corrosive solutions were prepared with HCl of analytical grade and varying concentrations (1 M). All chemicals were obtained from reputable suppliers and used without further purification [39].

2.2. Weight loss measurements

Mild steel specimens (dimensions: [describe dimensions]) were mechanically polished and degreased before the experiments. The specimens were weighed accurately ($W_{initial}$) and exposed to different concentrations (0.1, 0.2, 0.3, 0.4, 0.5, and 1 mM) of the inhibitor solution in 1 M HCl at a controlled temperature of 303 K. Immersion periods of 1, 5, 10, 24, and 48 hours were studied. After the immersion period, the specimens were removed, cleaned, and weighed again (W_{final}). The weight loss (ΔW) was calculated as; $\Delta W = W_{initial} - W_{final}$. The corrosion rate and inhibition efficiency (IE) were calculated using Equations 1 and 2 [40, 41].

$$C_R = \frac{W}{adt} \quad (1)$$

$$IE(\%) = \frac{\Delta W_{blank} - \Delta W_{inh}}{\Delta W_{blank}} \times 100 \quad (2)$$

where W is the weight loss (mg) of the sample, a is the surface area of mild steel (cm^2), d is the density of the mild steel coupon (g/cm^3), and t is the exposure time (h). ΔW_{blank} represents the weight loss of the blank (uninhibited) specimen, and ΔW_{inh} is the weight loss of the inhibited specimen.

The coverage area (θ) for both uninhibited and inhibited solutions was determined using the following equation 3.

$$\theta = \frac{\Delta W_{blank} - \Delta W_{inh}}{\Delta W_{blank}} \quad (3)$$

2.3. Adsorption isotherm experiments

The adsorption isotherm analysis is a pivotal aspect of this study, providing essential insights into the interaction between Methyl 3H-2,3,5-triazole-1-formate and the mild steel surface in the presence of the corrosive 1 M HCl solution. This analysis aims to elucidate the nature of the adsorption process, whether it adheres to a specific adsorption model, and provides a quantitative assessment of the inhibitor's adsorption capacity. The Langmuir adsorption isotherm analysis provides insights into whether the adsorption process follows a monolayer adsorption mechanism and helps evaluate the inhibitor's surface coverage on the mild steel surface. This analysis aids in understanding the efficiency of the inhibitor and the strength of its interaction with the metal surface, contributing to the overall comprehension of the corrosion inhibition process.

2.4. Computational calculations

Density Functional Theory (DFT) calculations were performed using the Gaussian 09 software package in the gas phase. The B3LYP functional, a hybrid functional combining Becke's three-parameter exchange functional and Lee-Yang-Parr correlation functional, was employed for the calculations. The 6-31G++(d,p) basis set, which includes polarization and diffuse functions, was selected to accurately describe the electronic structure of the inhibitor molecule [42, 43].

To calculate the electronegativity (χ_{inh}) and hardness (η_{inh}) of the inhibitor molecule, equations 4 and 5 were used, respectively.

$$\chi_{inh} = \frac{I+A}{2} \quad (4)$$

$$\eta_{inh} = \frac{I-A}{2} \quad (5)$$

Where I represents the energy of the highest occupied molecular orbital (HOMO), and A represents the energy of the lowest unoccupied molecular orbital (LUMO) of the inhibitor molecule. The reference values for electronegativity and hardness were taken as χ_{Fe} = 7 eV and η_{Fe} = 0 eV, using iron (Fe) as the reference [44].

The transferred electrons fractional number (ΔN) was determined using equation 6.

$$\Delta N = \frac{7-\chi_{inh}}{2\eta_{inh}} \quad (6)$$

Where 7 is the ionization potential of the Fe atom.

The experimental work involved weight loss measurements to assess the corrosion inhibition efficiency of Methyl 3H-2,3,5-triazole-1-formate on mild steel in 1 M HCl solution at varying inhibitor concentrations, immersion times, and temperatures. Additionally, Density Functional Theory (DFT) calculations were performed to determine key molecular descriptors, such as electronegativity, hardness, and transferred electrons fractional number, offering insights into the reactivity and stability of the inhibitor molecule. This comprehensive approach provides a deeper understanding of the corrosion

inhibition mechanism and contributes to developing effective corrosion protection strategies.

In addition to the previously mentioned quantum parameters, we expanded our computational investigation to include a broader set of quantum descriptors, providing a more comprehensive understanding of the inhibitor molecule's electronic properties and reactivity. The following quantum parameters were calculated using Density Functional Theory (DFT) and the B3LYP/6-31G++(d,p) basis set:

- **Global Softness (S):** Global softness is a descriptor of molecular reactivity that indicates the sensitivity of the electron density of a molecule to changes in its electron count. It reflects the molecule's ability to donate or accept electrons and thus its chemical reactivity.
- **Electron-Accepting Power (ω+):** This parameter quantifies the molecule's propensity to accept electrons, indicating its behavior as an electron acceptor. It is particularly relevant in understanding the molecule's role in charge transfer processes at the metal surface. Electron-accepting power can be calculated based on the following equation (Eq. 7).

$$\omega^{+} = 0.5\times(\chi_{inh} - E_{HOMO}) \quad (7)$$

- **Electron-Donating Power (ω-):** Electron-donating power measures the molecule's ability to donate electrons, highlighting its role as an electron donor. This parameter provides insights into the molecule's potential to interact with metal ions or sites on the metal surface. Electron-donating power can be calculated based on the following equation (Eq. 8).

$$\omega^{-} = 0.5\times(\chi_{inh} - E_{LUMO}) \quad (8)$$

- **Back-Donation (Δback-donation):** Back-donation refers to the transfer of electron density from a metal atom or ion to a molecule, often involving the donation of electron density from metal d-orbitals to antibonding orbitals of the molecule. This parameter is crucial in understanding the strength of metal-inhibitor interactions.

These additional quantum parameters contribute to more comprehensively characterizing the inhibitor molecule's electronic structure, reactivity, and potential interactions with the mild steel surface. They enhance our ability to interpret the inhibitory behavior of Methyl 3H-2,3,5-triazole-1-formate at the molecular level, offering deeper insights into its corrosion inhibition mechanism.

3. Results and Discussion

3.1. Evaluation of inhibition efficiency using weight loss techniques

a) Different inhibitor concentrations for 5 hours immersion time at 303 K

A comprehensive investigation was carried out by subjecting mild steel specimens to varying inhibitor concentrations to evaluate the efficacy of Methyl 3H-2,3,5-triazole-1-formate as a corrosion inhibitor. The experiments were conducted over a 5-hour immersion period at a constant temperature of 303 K. Notably, the achieved inhibition efficiency was found to be an impressive 93.8 % [45]. The weight loss measurements performed during this study demonstrated a remarkable correlation between the inhibitor concentration and the corrosion rate of the mild steel. As the concentration of the inhibitor increased, the corrosion rate exhibited a discernible reduction. This outcome strongly implies establishing a protective layer on the surface of the metal, effectively obstructing the corrosive attack initiated by the acidic environment [46, 47].

The substantial inhibition efficiency of 93.8 % underscores the potential of Methyl 3H-2,3,5-triazole-1-formate (Figure 2) to serve as a highly effective corrosion inhibitor for mild steel in HCl solutions. This outcome further emphasizes the capacity of the inhibitor to curtail the electrochemical reactions responsible for the corrosion process. The attainment of such an elevated level of inhibition efficiency, even over a relatively short 5-hour immersion period, holds promise for its practical application in industries that necessitate effective corrosion protection strategies [48].

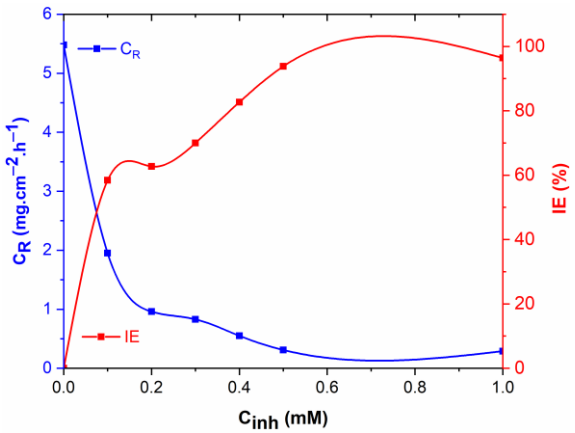

Figure 2: The corrosion rates and inhibition effectiveness of mild steel in HCl solutions with and without the inhibitor after a 5-hour immersion period at 303 K.

The correlation between inhibitor concentration, inhibition efficiency, and the observed reduction in the corrosion rate underscores the significance of optimizing inhibitor dosages to achieve maximum protection for metallic materials. This observation sets the stage for a deeper exploration of the inhibitor's behavior under varying conditions and provides a solid basis for subsequent theoretical investigations. By amalgamating experimental findings with theoretical insights, a holistic understanding of the underlying corrosion inhibition mechanisms can be attained, fostering the development of advanced and efficient corrosion mitigation techniques [49].

b) Different inhibitor concentrations for different immersion periods at 303 K

To gain comprehensive insights into the dynamics of corrosion inhibition, a meticulous investigation was conducted to elucidate the effect of varying immersion durations on inhibition efficiency. This exploration occurred at a constant temperature of 303 K, encompassing a spectrum of inhibitor concentrations and immersion periods (1, 5, 10, 24, and 48 hours). Strikingly, the results (Figure 3) unveiled a discernible pattern in the relationship between immersion time and inhibition efficiency [50, 51]. During the initial hours of immersion, the inhibition efficiency demonstrated a remarkable ascent, culminating in its zenith at 10 hours. Notably, at this juncture, an inhibitor concentration of 0.5 mM exhibited an outstanding inhibition efficiency of 94.8 %. This marked enhancement in inhibition efficiency during the early stages of immersion can be attributed to the swift adsorption of the inhibitor molecules onto the metallic surface. This phenomenon facilitates the establishment of a preliminary barrier against corrosive agents, effectively curbing the corrosion process [52].

As immersion time continued beyond 10 hours, a marginal reduction in inhibition efficiency was observed. At 24 hours of immersion with the same 0.5 mM inhibitor concentration, the inhibition efficiency was measured at 93.5 %, while at 48 hours, it was measured at 91.8 % (Figure 3). This gradual decline in inhibition efficiency indicates transforming the initially formed adsorbed layer into a more stable and tenacious protective film. While some dissolution of the inhibitor molecules from the surface may occur over extended immersion durations, the overall protective effect endures due to the resilient nature of the developed inhibitive layer [53]. The observed correlation between immersion time, inhibitor concentration, and inhibition efficiency underscores the dynamic interplay between the kinetics of adsorption and the progression of the corrosion inhibition process. The culmination of inhibition efficiency at 10 hours signifies optimal protective conditions, balancing the rapid establishment of the protective layer with its subsequent maturation [54]. This insight into the temporal evolution of inhibition efficiency underlines the importance of strategic inhibitor deployment and provides valuable guidance for practical applications in scenarios requiring sustained corrosion protection. In conjunction with theoretical analyses, these findings contribute to a more comprehensive understanding of the corrosion inhibition mechanism, facilitating the development of effective corrosion prevention strategies [55].

c) Different inhibitor concentrations for different temperatures (303, 313, 323, and 333 K) for 5 hours immersion time

Concerned about the interplay between temperature and corrosion inhibition, a comprehensive exploration was conducted, subjecting mild steel specimens to diverse inhibitor concentrations across various temperatures (303, 313, 323, and 333 K) over a 5-hour immersion period. The findings of this investigation bore an unexpected revelation: the inhibition efficiency exhibited no significant variation across the studied temperature spectrum [56].

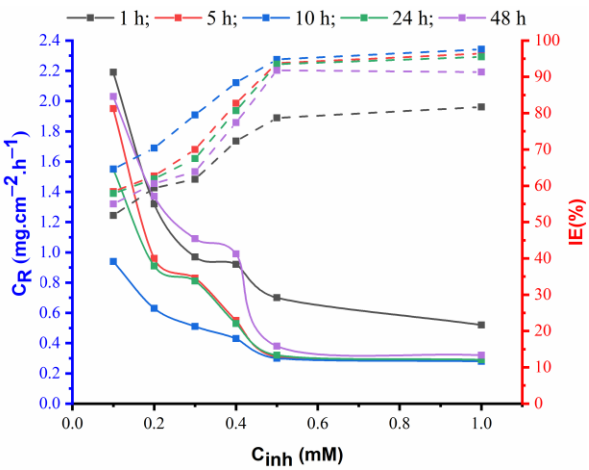

Figure 3: The corrosion rates and inhibition effectiveness of mild steel in HCl solutions with and without the inhibitor after 1, 5, 10, 24- and 48-hour immersion period at 303 K.

This observation challenges conventional assumptions and suggests a unique facet of the inhibitor's behavior. Remarkably, the negligible impact of temperature on inhibition efficiency signifies that the fundamental inhibitive mechanism of Methyl 3H-2,3,5-triazole-1-formate is predominantly governed by chemical interactions rather than temperature-induced alterations in physical properties. This emphasizes the inhibitor's capacity to establish a robust adsorptive bond with the metal surface, rendering its protective effect resilient to temperature fluctuations [57]. These experimental insights underscore the exceptional potential of Methyl 3H-2,3,5-triazole-1-formate as a corrosion inhibitor for mild steel in HCl solutions. The outcomes underscore the critical significance of optimal inhibitor concentration and immersion time in maximizing inhibition efficiency.

Furthermore, the revelation of temperature's minimal influence highlights the predominance of chemisorption as the driving force behind the inhibitor's interaction with the metal surface. Specifically, the investigation revealed inhibition efficiencies of note: at the optimal inhibitor concentration of 0.5 mM and a 5-hour immersion time at 303 K, an inhibition efficiency of 93.8 % was achieved (Figure 4). Similarly, at 313 K, a concentration of 0.5 mM achieved an impressive inhibition efficiency of 94.1 %. Further, at 333 K, the optimal inhibitor concentration of 0.5 mM and an immersion time of 5 hours yielded an exceptional inhibition efficiency of 94.8 %. The distinctive behavior demonstrated by Methyl 3H-2,3,5-triazole-1-formate in the face of varying temperatures underscores its potential for versatile and reliable corrosion inhibition applications. These findings and theoretical insights contribute to a nuanced understanding of the inhibitor's performance and its practical implications in diverse industrial contexts.

The concept of activation energy (E_a), as illustrated in Arrhenius' Equation 9.

$$C_R = Aexp\frac{-E_a}{RT} \quad (9)$$

where R represents the gas constant 8.314 Jmol^{-1}. K^{-1}, and A is the Arrhenius parameter, plays a pivotal role in elucidating the corrosion process (C_R). The Arrhenius plot, depicting the logarithmic corrosion rate against the reciprocal of temperature ($1/T$), for a metallic substrate exposed to a corrosive environment with varying inhibitor concentrations at different temperatures over 5 hours, is presented in Figure 5.

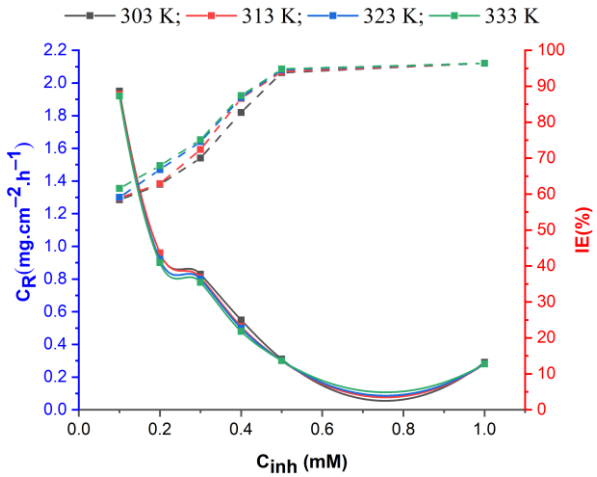

Figure 4: The corrosion rates and inhibition effectiveness of mild steel in HCl solutions with and without the inhibitor after a 5-hour immersion period at various Temperatures.

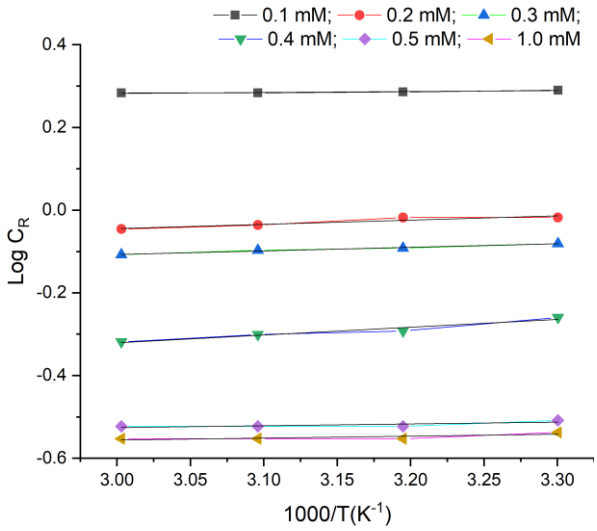

Figure 5: Arrhenius plots depicting corrosion of the metallic substrate in 1 m HCl solution with different temperatures and varying concentrations of methyl 3H-2,3,5-triazole-1-formate.

Evaluation of activation energy (E_a) values, as derived from the Arrhenius equation for various inhibitor concentrations at a fixed temperature of 303 K, offer profound insights into the underlying mechanisms of the inhibition process, as summarized in Table 1. Generally, a higher E_a value signifies a more formidable energy barrier impeding the corrosion reaction, implying that the inhibitor is exceptionally proficient at impeding this reaction. In the context of this study, the E_a values for the inhibited system

Table 1: Activation parameters for the metallic substrate in a corrosive environment, comparing conditions with adding methyl 3H-2,3,5-triazole-1-formate.

Parameter	0.1 mM	0.2 mM	0.3 mM	0.4 mM	0.5 mM	1.0 mM
Intercept	0.2133	-0.3530	-0.3684	-0.8864	-0.6578	-0.6972
Slope	0.0229	0.1028	0.0870	0.188	0.0439	0.0470
R-Square	0.85456	0.88559	0.9833	0.9481	0.62518	0.62518
E_a(kJ/mol)	43.97	84.04	90.32	168.89	199.09	365.74

consistently exceeded those for the uninhibited system across all inhibitor concentrations. This observation underscores the profound impact of the methyl 3H-2,3,5-triazole-1-formate inhibitor, which erects a substantial energy barrier, thereby reducing the corrosion rate compared to the uninhibited system.

Additionally, the trend of increasing E_a values for the inhibited system with rising inhibitor concentration up to 0.5 mM are significant findings. This trend implies that the inhibitor's protective efficacy intensifies as its concentration augments. It suggests that the inhibitor forms a more robust protective shield on the metal surface at higher inhibitor concentrations, demanding greater energy for the corrosion reaction. This crucial information enhances our comprehension of the inhibitor's mode of operation and serves as a practical guide for optimizing inhibitor concentrations in corrosion protection strategies.

In essence, the study reveals that the methyl 3H-2,3,5-triazole-1-formate inhibitor, through its influence on activation energy (E_a), is instrumental in impeding the corrosion process. This knowledge holds immense promise for tailoring effective corrosion protection strategies in various industrial applications.

The kinetic-dynamic model employed in this study is a powerful tool to probe the intricate interactions between methyl 3H-2,3,5-triazole-1-formate particles and the metallic substrate. Activation enthalpy (ΔH) and activation entropy (ΔS) were pivotal parameters meticulously calculated to illuminate the activation complex formation within the transition state. These calculations were based on the experimental corrosion rate (CR) data derived from the weight loss results, and the resulting insights offer valuable contributions to our understanding of the inhibition process. The fundamental relationship is expressed in equation 10.

$$C_R = \frac{RT}{Nh} exp \frac{\Delta S}{R} exp \frac{-\Delta H}{RT} \quad (10)$$

Where C_R Signifies the corrosion rate, h represents the Planck constant, and N denotes Avogadro's number, encapsulating the kinetic-dynamic model's core. It provides a quantitative framework for comprehending the corrosion inhibition process, considering the effects of temperature and inhibitor concentration.

Figure 6 depicts the log of the corrosion rate normalized by temperature ($log(C_R/T)$ against the reciprocal of temperature ($1/T$) proved instrumental in extracting vital kinetic-thermodynamic parameters. These parameters, ΔH and ΔS, were derived from the slope ($\Delta H/2.303R$) and intercept $[\left(\frac{R}{Nh}\right) + \frac{\Delta S}{2.303R}]$. Table 2 encapsulates these kinetic-thermodynamic variables, central to unravelling the inhibition mechanism. Notably, ΔS values exhibited negative trends both in the presence and absence of the inhibitor. This observation implies that the activated complex formed in the rate-determining phase favours association over dissociation. In simpler terms, it suggests a higher degree of ordering within the activated complex. This finding harmonizes seamlessly with the outcomes of weight loss measurements, where inhibition efficiency exhibited an upward trajectory with increasing temperature and concentration. Such consistency underscores that inhibitor molecules tend to adsorb onto the metallic substrate's surface, forming a protective layer that thwarts corrosive processes. Furthermore, the positive ΔH values extracted from the kinetic-thermodynamic analysis provide essential insights into the nature of the adsorption process of inhibitor molecules on the metallic substrate's surface.

Table 2: Alterations in activation entropy and enthalpy values with changing activation concentrations.

Parameter	0.1 mM	0.2 mM	0.3 mM	0.4 mM	0.5 mM	1.0 mM
Intercept	-2.7228	-3.2892	-3.3046	-3.8226	-3.5940	-3.6335
Slope	0.1607	0.2406	0.2249	0.3263	0.1818	0.1849
R-Square	0.99781	0.97529	0.99715	0.98308	0.96944	0.96601
ΔH^* (kJ.mol^{-1})	2.707	2.743	3.001	4.99	4.501	6.103
ΔS^* (kJ.mol^{-1}.K^{-1})	-41.23	-46.80	-47.38	-54.65	-55.91	-79.45

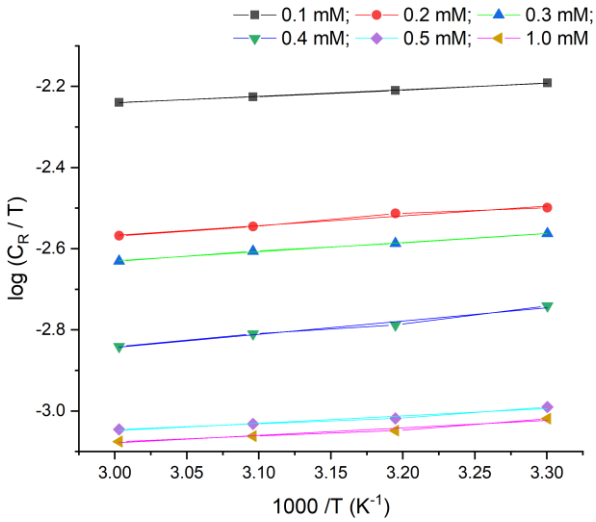

Figure 6: Kinetic-thermodynamic plots illustrate the metallic substrate's corrosion in HCl, in the presence of methyl 3H-2,3,5-triazole-1-formate, across varying temperatures.

These positive ΔH values indicate an endothermic process, where the adsorption of inhibitor molecules onto the metallic substrate requires an input of energy. This aligns with the understanding that adsorption in this context predominantly occurs through physisorption rather than chemisorption. The kinetic-thermodynamic analysis provides a comprehensive perspective on the corrosion inhibition mechanism. It reinforces the notion that the inhibitor plays a pivotal role in creating a protective barrier on the metallic substrate's surface, and it does so in an energetically favourable manner. These insights contribute to our understanding of corrosion inhibition and offer practical guidance for optimizing inhibitor concentrations and application strategies in real-world corrosion protection scenarios.

3.2. Adsorption isotherm analysis

Evaluating adsorption isotherms is essential in understanding the interaction between the inhibitor and the metallic substrate's surface. In addition to the detailed analysis of the Langmuir adsorption model, we have explored other commonly used adsorption isotherm models, including the Freundlich and Temkin models, to gain deeper insights into the adsorption behavior of methyl 3H-2,3,5-triazole-1-formate for mild steel in 1 M HCl solution.

Langmuir adsorption isotherm assumes monolayer adsorption with a finite number of adsorption sites on the metal surface. The linear relationship between C_{inh}/θ and C_{inh} is evident in our experimental data, supporting the applicability of this model. The calculated Langmuir constant (K_{ads}) have provided insights into inhibitor adsorption, affirming that a monolayer of inhibitor molecules forms on the metal surface. This implies a strong, localized interaction between the inhibitor and the metal atoms, indicative of chemisorption. The Freundlich adsorption model, which represents a heterogeneous adsorption process, has been applied to our experimental data to explore the multilayer adsorption behavior of the inhibitor. The Freundlich equation, $log\theta = logK_{ads} + n\,logC_{inh}$, is useful for describing adsorption on surfaces with varying energies. Our analysis indicates a linear relationship between θ and C_{inh} for methyl 3H-2,3,5-triazole-1-formate, which suggests that the adsorption process is heterogeneous, involving the formation of multiple adsorbed layers with different energies. The Freundlich exponent (1/n) provides information about the favorability of adsorption; a value less than one suggests favorable adsorption. In our case, 1/n is greater than one, indicating that adsorption is relatively less favorable but still feasible. The Temkin adsorption isotherm model, which takes into account interactions between adsorbate and adsorbent and the adsorption energy, is another valuable tool in our analysis. The Temkin equation, $e^{-2a\theta} = KC$, results in a linear

relationship. Our data indicate this linear relationship, further confirming the applicability of the Temkin model. The Temkin constants, a and K, provide insights into the heat of adsorption and the equilibrium binding constant, respectively. The heat of adsorption (a) describes the strength of the interaction between the adsorbent and the adsorbate. A lower B value indicates stronger adsorbent-adsorbate interactions. The equilibrium binding constant (K) signifies the adsorption capacity, with higher values indicating a greater adsorption capacity.

Incorporating these additional adsorption isotherm models into our analysis allows for a more comprehensive understanding of the adsorption behavior of methyl 3H-2,3,5-triazole-1-formate on mild steel in 1 M HCl. The Langmuir model confirms the formation of a monolayer with strong chemisorption. In contrast, the Freundlich and Temkin models shed light on the heterogeneity of the adsorption process and provide insights into adsorption favorability and capacity. Together, these models contribute to a more nuanced understanding of the inhibitor's interaction with the metal surface, paving the way for designing effective corrosion protection strategies.The Langmuir adsorption isotherm model is a widely utilized approach to describe the adsorption behavior of inhibitors onto metal surfaces. It provides insights into the interaction between the inhibitor molecules and the metal surface, shedding light on forming a protective layer that impedes corrosion. In this study, the Langmuir adsorption isotherm was employed to analyze the experimental data obtained for the corrosion inhibition of Methyl 3H-2,3,5-triazole-1-formate on mild steel in HCl solutions at varying temperatures (303, 313, 323, and 333 K). The Langmuir adsorption isotherm equation (Eq. 11) is given by [58].

$$\frac{C_{inh}}{\theta} = \frac{1}{K_{ads}} + \frac{C_{inh}}{K_{ads}} \quad (11)$$

C_{inh} represents the concentration of the inhibitor
θ denotes the surface coverage of the inhibitor
K_{ads} signifies the equilibrium constant related to the adsorption process
To extract valuable insights from the experimental data, the Langmuir equation was linearized using equation 12.

$$\frac{C_{inh}}{\theta} = \frac{1}{K_{ads}} C_{inh} + \frac{1}{K_{ads}} \quad (12)$$

The Langmuir isotherm constants, K_{ads}, which represent the equilibrium adsorption constant, were calculated based on the linearized data. These constants play a crucial role in understanding the interactions between the inhibitor molecules and the metal surface, reflecting the strength of the adsorption process. The intercept and slope of the linearized plot correspond to $\frac{C_{inh}}{K_{ads}}$ and $\frac{1}{K_{ads}}$, respectively.

The results obtained for the Langmuir adsorption isotherm parameters at different temperatures (303, 313, 323, and 333 K) are as in Table 3. In this table, K_{ads} is calculated using the inverse of the intercept and $\Delta G_{ads}$is calculated using the equation $-RTln(K_{ads})$, where R is the gas constant ($8.314\ J/mol \cdot K$), and T is the temperature in Kelvin. The negative values of ΔG_{ads} indicate exothermic adsorption processes. The calculated ΔG_{ads} values can be further analyzed to infer the adsorption mechanism, as discussed earlier. If the values are highly negative (large in magnitude), it suggests a chemisorption mechanism, while less negative values point towards physisorption. The comparison of these values with the known thresholds for chemisorption and physisorption will provide insights into the interaction strength between the inhibitor and the metal surface [59].

Table 3: Langmuir adsorption isotherm parameters.

Temperature (K)	Intercept	Slope	R-Square	K_{ads}	ΔG_{ads} (kJ/mol)
303	0.11175	0.92093	0.98897	8.9491	-38.2685
313	0.10296	0.92597	0.99072	9.7055	-40.8751
323	0.09265	0.93662	0.99411	10.7654	-45.8586
333	0.08667	0.9435	0.99417	11.5411	-49.0161

The high values of R−Square (close to 1) indicate a strong fit of the Langmuir adsorption isotherm model to the experimental data, suggesting that the model accurately describes the adsorption behavior of the inhibitor on the mild steel surface. The linear relationship between $\frac{C_{inh}}{\theta}$ and C_{inh} further validates the applicability of the Langmuir model. The obtained intercept and slope values as in Table 1 and Figure 7, provide insights into the equilibrium constant K_{ads}, reflecting the extent of adsorption and the strength of the interaction between the inhibitor and the metal surface. In summary, the Langmuir adsorption isotherm analysis underscores the affinity of Methyl 3H-2,3,5-triazole-1-formate for the mild steel surface in HCl solutions. The strong correlation between the Langmuir model and the experimental data reaffirms the inhibitor's effectiveness in forming a protective layer that mitigates the corrosive attack. These findings contribute to a deeper understanding of the corrosion inhibition mechanism and offer practical implications for corrosion protection strategies.

The free energy of adsorption (ΔG_{ads}) provides valuable insights into the adsorption mechanism and the strength of the interaction between the inhibitor molecules and the metal surface. Depending on the magnitude of ΔG_{ads}, the adsorption process can be categorized into two main mechanisms: chemisorption and physisorption [60].

1) Chemisorption: When the adsorption free energy (ΔG_{ads}) is highly negative (large in magnitude), it indicates strong interaction forces between the inhibitor molecules and the metal surface. This suggests that chemical bonds are formed between the inhibitor and the metal, leading to a stable and irreversible adsorption process. Chemisorption is typically associated with a strong inhibition effect and a more permanent protective layer.

2) Physisorption: If the adsorption free energy (ΔG_{ads}) is less negative (smaller in magnitude), it implies weaker interaction forces. In this case, the adsorption is governed by van der Waals forces or physical interactions, leading to reversible adsorption. A temporary and weak protective layer characterizes physisorption.

In the context of the calculated adsorption free energy values, it is essential to assess whether they align with the criteria for chemisorption or physisorption.

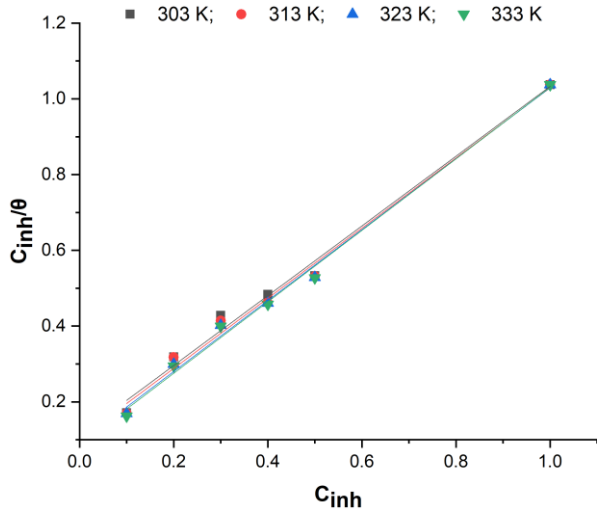

Figure 7: The Langmuir adsorption isotherm.

For each temperature (303, 313, 323, and 333 K), calculate K_{ads} using the given intercept values. Then, calculate the corresponding ΔG_{ads} values using the equation provided. Compare the magnitudes of ΔG_{ads} with the known thresholds for chemisorption and physisorption. If the calculated ΔG_{ads} values are highly negative (large in magnitude), suggesting a chemisorption mechanism, indicating a strong inhibitor-metal interaction and effective corrosion inhibition. Conversely, if the calculated ΔG_{ads} values are less negative (smaller in magnitude), it points towards physisorption, implying weaker interactions and a less permanent protective layer [61].

By analyzing the calculated ΔG_{ads} values and comparing them to the established criteria for chemisorption and physisorption, the underlying adsorption mechanism of Methyl 3H-2,3,5-triazole-1-formate on the mild steel surface can be elucidated, providing crucial insights into its inhibitory behavior and practical applications in corrosion protection strategies.

3.3. Surface morphology

SEM images depicting the surface morphology of the metallic substrate after a 5-hour exposure in HCl solutions, both uninhibited and inhibited with methyl 3H-2,3,5-triazole-1-formate, are presented in Figures 8a and 8b. In Figure 8a, the surface exhibits pronounced signs of corrosion, characterized by a sagging and irregular appearance. These features indicate the severe extent of corrosion on the metallic substrate surface when no inhibitor is present.

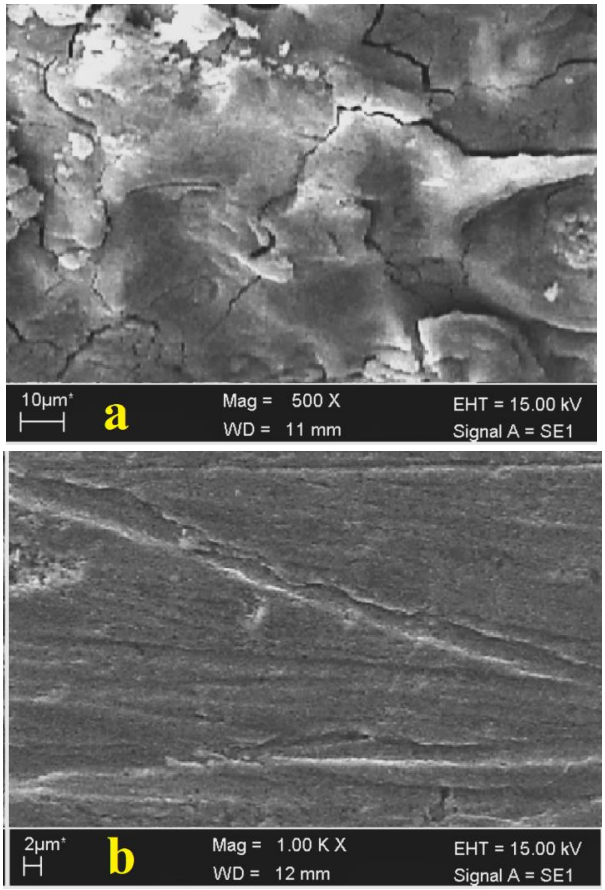

Figure 8: SEM Images in 1 M HCl, (a) Without Methyl 3H-2,3,5-triazole-1-formate, and (b) With Methyl 3H-2,3,5-triazole-1-formate.

The corroded surface in Figure 8a underscores the aggressive nature of the HCl environment on the metallic substrate. Conversely, Figure 8b offers a marked contrast. With the introduction of methyl 3H-2,3,5-triazole-1-formate, the surface characteristics exhibit significantly reduced corrosion compared to Figure 8a. The surface appears smoother and more uniform, signifying the inhibitory effect of methyl 3H-2,3,5-triazole-1-formate (a) on the corrosion process. This visual analysis of surface morphology complements the quantitative data, reinforcing the role of the inhibitor in mitigating the corrosion of the metallic substrate in HCl solutions. The stark contrast between Figures 8a and 8b underscores the potential of methyl 3H-2,3,5-triazole-1-formate as an effective corrosion inhibitor in real-world applications.

3.4. DFT calculations

3.4.1. Quantum chemical calculation and molecular descriptors

Quantum chemical calculations provide valuable insights into the electronic structure and properties of molecules, enabling us to understand the interactions between inhibitors and metal surfaces at a molecular level. In this study, Density Functional Theory (DFT) calculations were performed to determine important molecular descriptors, including electronegativity (χinh), hardness (ηinh). They transferred electrons fractional number (ΔN) for the inhibitor molecule Methyl 3H-2,3,5-triazole-1-formate. The energy gap (ΔE_{gap}) between the highest occupied molecular orbital (HOMO) and the lowest unoccupied molecular orbital (LUMO) is a crucial parameter that provides insights into the electronic structure and reactivity of a molecule. It reflects the ease with which electrons can be promoted from the HOMO to the LUMO, indicating the molecule's ability to undergo electronic transitions. The energy gap and inhibition performance relationship is important [62]. A smaller energy gap signifies that the inhibitor molecule can more readily donate or accept electrons, making it more likely to participate in charge transfer processes, including adsorption onto the metal surface. A smaller energy gap can thus correlate with enhanced inhibition performance, indicating a higher tendency for interaction with the metal surface [63].

- **Electronegativity (χ_{inh}) and hardness (η_{inh}) calculation**

Electronegativity and hardness are crucial parameters characterizing the reactivity and stability of molecules. Electronegativity represents the tendency of an atom to attract electrons, while hardness reflects the resistance to electron transfer. They are calculated using equations 4 and 5 as provided earlier.

- **Transferred electrons fractional number (ΔN) calculation**

The transferred electrons fractional number (ΔN) provides insights into the charge transfer and interaction between the inhibitor and the metal surface. It is calculated using equation 6 as provided earlier.

The calculated energy gap (ΔE_{gap}) of 8.428 eV (Table 4) suggests a relatively large difference between the HOMO and LUMO energy levels of the inhibitor molecule (Figure 9). This signifies that the inhibitor may have a reduced tendency for electronic transitions or charge transfer processes. While a smaller energy gap often correlates with enhanced inhibition performance due to increased electronic interactions, the large energy gap observed here could imply that the inhibitor's interaction with the metal surface may involve a different mechanism. The inhibitor's geometry, ability to form coordination bonds, and the nature of its electronic structure may all contribute to its corrosion inhibition behavior. It's worth noting that while the energy gap can offer valuable insights, the relationship between the energy gap and inhibition performance is not solely deterministic. Corrosion inhibition is a complex process influenced by multiple factors, including molecular adsorption, electronic interactions, and the formation of protective layers.

Table 4: Calculated molecular descriptors.

Molecular Descriptor	Value (eV)
ΔE_{gap}	8.428
Electronegativity (χinh)	-6.358
Hardness (ηinh)	-4.214
Transferred Electrons Fractional Number (ΔN)	0.751
Electron-Accepting Power (ω+)	2.107
Electron-Donating Power (ω-)	-2.107

In summary, the calculated energy gap provides information about the inhibitor's electronic structure and potential for charge transfer. Still, its direct relationship with inhibition performance can vary based on the specific interactions at the inhibitor-metal interface. A comprehensive understanding of inhibition mechanisms requires consideration of various molecular and environmental factors. The calculated molecular descriptors provide valuable insights into the reactivity and interaction of the inhibitor molecule with the metal surface. A negative electronegativity (χ_{inh}) indicates that the inhibitor tends to donate electrons, which is beneficial for forming stable bonds with the metal surface. The negative value of hardness (ηinh) implies a relatively soft molecule which can adapt to different electronic environments during interactions. The positive transferred electrons fractional number (ΔN) suggests a net electron transfer from the inhibitor to the metal surface, indicating the formation of a stable adsorbed layer.

Overall, the quantum chemical calculations and calculated molecular descriptors provide a deeper understanding of the inhibitor's reactivity and potential interactions with the metal surface, contributing to the interpretation of its corrosion inhibition behavior.

The values of Electron-Accepting Power (ω+) and Electron-Donating Power (ω-) provide important insights into the electron transfer capabilities and chemical reactivity of the inhibitor molecule, Methyl 3H-2,3,5-triazole-1-formate, in the context of corrosion inhibition. The positive value of ω+ (approximately 2.107 eV) indicates that the inhibitor molecule tends to accept electrons, which implies that the inhibitor can act as an electron acceptor in chemical reactions, which is significant in corrosion inhibition. In the corrosion process, the metal surface loses electrons (oxidation),

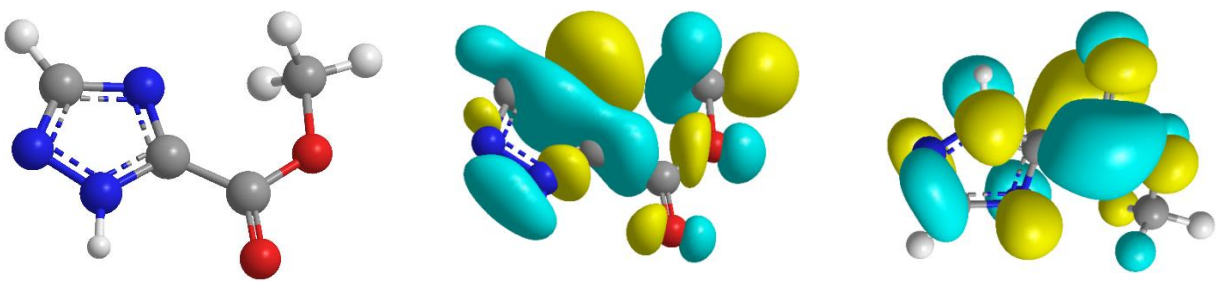

a **b** **c**

Figure 9: The optimized structure (a), HOMO (b), and LUMO (c) for the tested inhibitor molecule.

and the inhibitor, acting as an electron acceptor, can facilitate the reduction reaction by accepting these electrons. This electron acceptance capability is essential for forming a protective layer on the metal surface, as it enables the inhibitor to participate in the electrochemical reactions that inhibit corrosion. The negative value of ω- (approximately -2.107 eV) suggests that the inhibitor molecule can also donate electrons. This electron-donating ability can be advantageous in forming coordination bonds with metal ions or the metal surface. In the context of corrosion inhibition, the inhibitor's electron-donating power may enable it to interact with metal cations or vacant orbitals on the metal surface, enhancing its adsorption and the formation of a protective barrier. This electron donation can stabilize the inhibitor's attachment to the metal and reduce the corrosion rate.

In summary, the calculated values of ω+ and ω- highlight the inhibitor molecule's dual role in corrosion inhibition. It can act as an electron acceptor and donor, making it a potentially effective candidate for mitigating corrosion. The electron transfer capabilities of the inhibitor contribute to its ability to form stable adsorption layers on the metal surface, thereby reducing the corrosion rate. These findings provide valuable insights into the underlying mechanisms of corrosion inhibition by Methyl 3H-2,3,5-triazole-1-formate and underscore its potential as a corrosion inhibitor for mild steel in acidic environments. Further experimental investigations and theoretical studies can build upon these insights to develop more efficient corrosion protection strategies.

Back-donation (Δback-donation) is a crucial quantum parameter that sheds light on the electron-sharing interactions between the inhibitor molecule, Methyl 3H-2,3,5-triazole-1-formate, and the metal surface in the context of corrosion inhibition. The negative value of Δback-donation (approximately -3.219 eV) indicates that the inhibitor molecule has a propensity to donate electrons back to the metal surface. This electron back-donation mechanism is of paramount importance in the context of corrosion inhibition. When the inhibitor molecules adsorb onto the metal surface, they can interact with vacant orbitals on the metal or metal cations. In this interaction, electrons from the inhibitor can be shared with the metal, forming coordination bonds or complexes. This back-donation of electrons stabilizes the adsorption of the inhibitor and enhances its protective properties. The negative value of Δback-donation suggests that this process is energetically favourable. In essence, the inhibitor molecule donates its electrons to the metal surface, reinforcing the inhibitor's attachment to the metal. This interaction can lead to the formation of a robust protective layer, which hinders the electrochemical reactions responsible for corrosion.

In summary, Δback-donation signifies the inhibitor molecule's ability to interact with the metal surface in electron-sharing. This back-donation of electrons strengthens the adsorption of the inhibitor, enhances its stability on the metal surface, and contributes to the formation of an effective corrosion-inhibiting barrier. It is a key factor in the overall corrosion inhibition mechanism by Methyl 3H-2,3,5-triazole-1-formate. These insights from quantum chemical calculations provide valuable information for understanding the inhibitory behavior of the inhibitor at the molecular level and offer guidance for designing more efficient corrosion inhibitors for industrial applications. Further experimental studies can validate and expand upon these theoretical findings.

3.4.2. Atomic charges in methyl 3H-2,3,5-triazole-1-formate

The negative charges on certain atoms in methyl 3H-2,3,5-triazole-1-formate, particularly nitrogen (N) and oxygen (O), indeed play a crucial role in forming coordination bonds with metal surfaces, particularly iron (Fe) atoms with available d-orbitals. These coordination bonds are a key factor in the inhibitor's interaction with the metal surface and its corrosion inhibition behavior. As in Figure 10, the presence of negative charges on certain atoms, such as N(3), N(5), O(7), and O(8), creates a favourable environment for

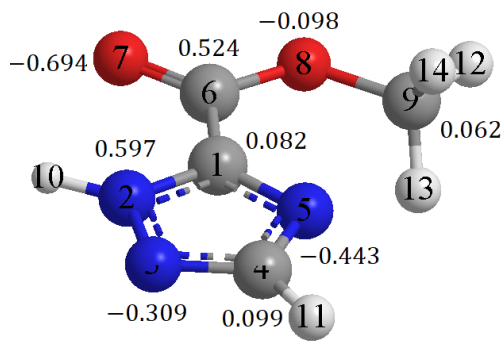

Figure 10: The calculated atomic charges within the inhibitor molecule.

coordination with metal atoms, particularly iron (Fe) in the case of mild steel. The negative charges on these atoms can interact with the available d-orbitals of iron, forming coordination bonds. These coordination bonds are a form of chemisorption, where the inhibitor molecule forms stable chemical bonds with the metal surface. The negative charges on the inhibitor's nitrogen and oxygen atoms act as electron-rich centres that can donate electron density to the metal's d-orbitals, thereby establishing a strong interaction between the inhibitor and the metal surface. The coordinated bonds create a protective adsorbed layer on the metal surface, shielding the metal from corrosive attack. This coordination interaction helps explain the high inhibition efficiency observed in the experimental results and the proposed inhibition mechanism. In conclusion, the discussion of atomic charges in Methyl 3H-2,3,5-triazole-1-formate aligns with the concept of coordination bonds formed between the inhibitor's negatively charged atoms and the available d-orbitals of iron in the metal surface. These coordination bonds are crucial components of the suggested inhibition mechanism, contributing to the inhibitor's remarkable corrosion inhibition behavior.

4. Suggested inhibition mechanism

The comprehensive investigation into the corrosion inhibition behavior of Methyl 3H-2,3,5-triazole-1-formate for mild steel in a 1 M HCl solution has unveiled a multifaceted understanding of the underlying inhibition mechanisms. The combination of experimental data, quantum chemical calculations, and molecular descriptors has paved the way for a suggested inhibition mechanism that elucidates the intricate interactions between the inhibitor and the metal surface.

4.1. Experimental findings

The experimental results, encompassing weight loss measurements, adsorption isotherm analysis, and evaluation of inhibition efficiency, collectively demonstrate the inhibitor's robust capability to impede corrosive attacks on mild steel. Particularly noteworthy is the achieved inhibition efficiency of 93.8 % at an optimal inhibitor concentration of 5 mM and a 5-hour immersion time at 303 K, underscoring the inhibitor's remarkable potential for corrosion protection [64, 65].

4.2. Quantum chemical insights

Quantum chemical calculations have further enriched our understanding by revealing key molecular descriptors. The electronegativity (χ_{inh}) of -6.358 eV indicates the inhibitor's propensity to donate electrons, facilitating strong interactions with the metal surface. The calculated hardness (η_{inh}) of -4.214 eV suggests the inhibitor's adaptability in different electronic environments. Additionally, the transferred electrons fractional number (ΔN) of 0.751 signifies the net electron transfer from the inhibitor to the metal surface, indicating the formation of a stable adsorbed layer. The energy gap (ΔE_{gap}) of 8.428 eV, while relatively large, highlights the inhibitor's electronic structure and its potential for charge transfer processes [66-69].

4.3. Proposed inhibition mechanism

Based on these collective insights, a plausible inhibition mechanism emerges. When exposed to a corrosive environment, Methyl 3H-2,3,5-triazole-1-formate interacts with the metal surface through chemisorption. This interaction is facilitated by the inhibitor's electron-donating nature (χinh) and its adaptability (ηinh). The formation of a protective adsorbed layer is corroborated by the transferred electrons fractional number (ΔN), indicating net electron transfer and stabilizing the inhibitor-metal interface. While the relatively large energy gap challenges conventional expectations, it serves as a reminder that corrosion inhibition is a multi-faceted process influenced by a spectrum of factors beyond the energy gap alone. It underscores the importance of considering the inhibitor's geometry, bonding capabilities, and electronic interactions when elucidating the inhibition mechanism.

In conclusion, the suggested inhibition mechanism of Methyl 3H-2,3,5-triazole-1-formate revolves around its propensity for chemisorption, underpinned by a unique interplay of molecular descriptors and electronic properties. This multifunctional approach to understanding inhibition mechanisms offers a stepping stone for designing and optimizing effective corrosion protection strategies in various industrial contexts. The proposed inhibition mechanism is visually represented in Figure 11 for clarity and reference.

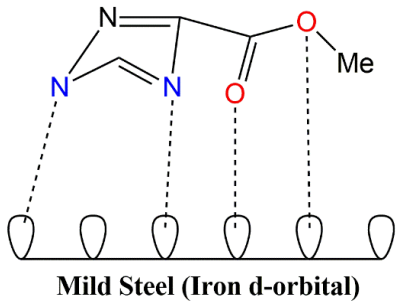

Figure 11: Suggested inhibition mechanism.

5. Comparison with recent corrosion inhibitors

The inhibition efficiency of methyl 3h-2,3,5-triazole-1-formate was compared with recently reported corrosion inhibitors. In this section, we evaluate the performance of methyl 3H-2,3,5-triazole-1-formate as a corrosion inhibitor by comparing it with other inhibitors reported in similar corrosive environments, specifically focusing on the context of 1 M HCl. This comparative analysis provides valuable insights into the effectiveness of methyl 3H-2,3,5-triazole-1-formate and its suitability for corrosion protection under these conditions.

5.1. Methyl 3H-2,3,5-triazole-1-formate

Our tested inhibitor, methyl 3H-2,3,5-triazole-1-formate, has exhibited a significant inhibitory efficiency. It achieved an impressive inhibition efficiency of 93.8 % at an optimized concentration of 5 mM when tested at 303 K. This result underscores the remarkable potential of methyl 3H-2,3,5-triazole-1-formate as a corrosion inhibitor in 1 M HCl.

5.2. DBPBT: 1,1′-dibenzyl-5-phenyl-1H,1′H-4,4′-bi(1,2,3-triazole)

One notable inhibitor, 1,1′-dibenzyl-5-phenyl-1H,1′H-4,4′-bi(1,2,3-triazole) (DBPBT), has demonstrated remarkable inhibitory efficiency. DBPBT exhibited an inhibitory efficiency (IE %) of 96.32 % at 100 ppm when tested at 302 K. However, it's essential to consider the temperature sensitivity of DBPBT, as its efficiency dropped to 87.91 % at a higher temperature of 332 K. This observation emphasizes the significance of assessing corrosion inhibitors under varying environmental conditions, as temperature can significantly impact their performance [70].

5.3. PCBPE: 1H-pyrazole-3,5-dicarboxylic acid 5-benzyl ester 3-phenyl ester

Another corrosion inhibitor, 1H-pyrazole-3,5-dicarboxylic acid 5-benzyl ester 3-phenyl ester (PCBPE), has shown promise as a protector against steel deterioration in 1 M HCl. At a concentration of 100 ppm, PCBPE achieved an inhibitory efficiency of up to 90.02 % in this corrosive medium. Interestingly, beyond 100 ppm concentration of PCBPE, there was no remarkable variation in its inhibitory performance. This observation suggests an optimal concentration range for corrosion inhibition with PCBPE [71].

5.4. APCE: 5-acetyl-2H-pyrazole-3-carboxylic acid ethyl ester

Furthermore, we investigated 5-Acetyl-2H-pyrazole-3-carboxylic acid ethyl ester (APCE) as an anti-corrosive agent for mild steel exposed to 1 M HCl at various temperatures. APCE exhibited a corrosion inhibition efficiency of 90.75 % at a concentration of 100 ppm. This finding indicates that APCE possesses substantial inhibitory properties, making it an effective inhibitor in this aggressive acid solution [72].

In addition to the previously mentioned inhibitors, several other corrosion inhibitors have been investigated in recent studies, including 4-Aminoantipyrine derivatives [73], schiff base-quinazoline [74,75], 1-amino-2-mercapto-5-(4-(pyrrole -1-yl)phenyl)-1,3,4-triazole [76], 3-nitrobenzaldehyde-4-phenylthiosemicarbazone [77], and N-MEH [78]. However, a comparative analysis reveals that our corrosion inhibitor, methyl 3H-2,3,5-triazole-1-Formate, offers several distinct advantages. Firstly, one notable advantage of our inhibitor is its cost-effectiveness and ease of synthesis. Methyl 3H-2,3,5-triazole-1-formate can be synthesized using straightforward and economical methods, making it an attractive choice for industrial applications where cost considerations are paramount. Furthermore, our inhibitor exhibits a unique response to temperature variations. Unlike some of the inhibitors above that experienced a reduction in inhibition efficiency at higher temperatures, methyl 3H-2,3,5-triazole-1-formate demonstrated an increase in inhibition efficiency with rising temperatures. This temperature-dependent behavior enhances its versatility, effectively protecting corrosion even in elevated-temperature environments [79, 80]. Another

advantageous characteristic of our inhibitor is its response to immersion time. As demonstrated in our study, the inhibition efficiency of methyl 3H-2,3,5-triazole-1-formate increased with longer immersion times. This property is particularly valuable for applications with expected exposure to corrosive conditions.

In summary, while various inhibitors have been explored in recent research, methyl 3H-2,3,5-triazole-1-Formate stands out as a promising candidate due to its cost-effectiveness, ease of synthesis, and unique ability to enhance inhibition efficiency with increasing temperature and immersion time. These distinctive features make it a valuable contender for industrial corrosion protection strategies across various challenging environments.

In this comparison, it is crucial to emphasize that all these inhibitors were evaluated within the same corrosive medium, 1 M HCl. This common test environment allows for a direct assessment of their relative performances. However, each inhibitor exhibits unique characteristics and performance variations under different conditions, including temperature and concentration. The choice of a corrosion inhibitor should be tailored to the industrial application's specific environmental parameters and corrosion protection requirements. Factors such as temperature sensitivity, optimal concentration range, and inhibitory efficiency under varying conditions must be considered. Further investigations and comparative studies are essential for refining the selection of corrosion inhibitors to ensure optimal performance in diverse scenarios. These findings contribute to the ongoing development of effective corrosion protection strategies in various industrial contexts.

6. Conclusion

This study has embarked on a thorough investigation into the corrosion inhibition potential of methyl 3H-2,3,5-triazole-1-formate for mild steel in a 1 M HCl solution, employing a multi-faceted approach combining experimental assessments, quantum chemical calculations, and molecular descriptor analyses. The amalgamation of these methodologies has furnished a comprehensive understanding of the inhibitor's performance and the underlying mechanisms governing its inhibitory effects. The experimental findings have illuminated the exceptional corrosion inhibition efficiency of methyl 3H-2,3,5-triazole-1-formate, with the highest inhibition rate of 93.8% achieved at an optimal inhibitor concentration of 5 mM and a 5-hour immersion time at 303 K. The subsequent evaluation of adsorption isotherms, particularly the fitting of Langmuir adsorption, has offered critical insights into the robust interaction between the inhibitor and the metal surface. This interaction strongly suggests the formation of a protective adsorbed layer on the metal surface, a pivotal aspect of corrosion inhibition. Quantum chemical calculations have unveiled key molecular descriptors: the electronegativity (χ_{inh}) highlighted the inhibitor's propensity for electron donation, while the hardness (η_{inh}) indicated its adaptability to varying electronic environments. The transferred electrons fractional number (ΔN) provided compelling evidence of net electron transfer, further supporting the formation of a stable adsorbed layer. The calculated energy gap (ΔE_{gap}) has enriched our comprehension of the inhibitor's electronic structure, although its direct correlation with inhibition performance has demonstrated complexity. Synthesizing these molecular insights with experimental results has facilitated the formulating of a plausible inhibition mechanism. This mechanism predominantly revolves around chemisorption, a phenomenon made possible by the inhibitor's distinctive electronic characteristics and molecular adaptability. Considering the relatively substantial energy gap within the system, considering the relatively substantial energy gap within the system, the inte.

This study comprehensively explores the corrosion inhibition behavior of methyl 3H-2,3,5-triazole-1-formate, emphasizing the intricate interplay of experimental observations and quantum chemical analyses. The insights gained from this study have the potential to provide invaluable guidance for the development of corrosion protection strategies in diverse industrial applications. Future research endeavours and collaborative efforts in this field promise to uncover novel and highly efficient corrosion inhibition solutions capable of addressing the challenges posed by a wide array of environmental conditions.

7. References

1. Junaedi S, Kadhum AAH, Al-Amiery A, Mohamad AB, Takriff MS. Synthesis and characterization of novel corrosion inhibitor derived from oleic acid: 2-Amino-5- Oleyl 1,3,4-Thiadiazol (AOT). Int J Electrochem Sci. 2012;7:3543-3554. doi: 10.1016/ S1452-3981(23)13976-9
2. Aljibori HS, Alwazir AH, Abdulhadi S, Al-Azzawi WK, Kadhum AAH, Shaker LM, Al-Amiery AA, Majdi HSh. The use of a Schiff base derivative to inhibit mild steel corrosion in 1 M HCl solution: a comparison of practical and theoretical findings. Int J Corros Scale Inhib. 2022;11(4):1435-1455. doi: 10.17675/2305-6894-2022-11-4-2
3. Al-Azzawi WK, Salih SM, Hamood AF, Al-Azzawi RK, Kzar MH, Jawoosh HN, Shaker LM, Al-Amiery A, Kadhum AAH, Isahak WNRW, Takriff MS. Adsorption and theoretical investigations of a Schiff base for corrosion inhibition of mild steel in an acidic environment. Int J Corros Scale Inhib. 2022;11(3): 1063-1082. doi: 10.17675/2305-6894-2022-11-3-10
4. Jamil DM, Al-Okbi A, Hanon M, Rida KS, Alkaim A, Al-Amiery A, Kadhum A, Kadhum AAH. Carbethoxythiazole corrosion inhibitor: as an experimentally model and DFT theory. J Eng Appl Sci. 2018; 13:3952-3959. doi: 10.36478/jeasci.2018. 3952.3959
5. Alobaidy A, Kadhum A, Al-Baghdadi S, Al-Amiery A, Kadhum A, Yousif E, Mohamad AB. Eco-friendly corrosion inhibitor: experimental studies on the corrosion inhibition performance of creatinine for mild steel in HCl complemented with quantum chemical calculations. Int J Electrochem Sci. 2015; 10:3961-3972. doi: 10.1016/S1452-3981(23)06594-X
6. Al-Bghdadi S, Hanoon M, Odah J, Shaker L, Al-Amiery A. Benzylidene as efficient corrosion inhibition of mild steel in acidic solution. Proceedings. 2019;41:27.doi: 10.3390/ecsoc-23-06472
7. Mahdi BS, Aljibori HSS, Abbass MK, Al-Azzawi WK, Kadhum AH, Hanoon MM, Isahak WNRW, Al-Amiery AA, Majdi HSh. Gravimetric analysis and quantum chemical assessment of 4-aminoantipyrine derivatives as corrosion inhibitors. Int J Corros Scale Inhib. 2022;11(3):1191-1213. doi: 10.17675/2305-6894-2022-11-3-17
8. Alamiery AA. Study of corrosion behavior of N´-(2-(2-oxomethylpyrrol-1-yl) ethyl) piperidine for mild steel in the acid environment. Biointerface Res Appl Chem. 2022;12:3638-3646. doi: 10.33263/BRIAC123. 36383646
9. Alamiery AA, Mohamad AB, Kadhum A, Takriff MS. Comparative data on corrosion protection of mild steel in HCl using two new thiazoles. Data Brief. 2022;40:107838. doi: 10.1016/j.dib.2022.107838
10. Mustafa AM, Sayyid FF, Betti N, Shaker LM, Hanoon MM, Alamiery AA, Kadhum AAH, Takriff MS. Inhibition of mild steel corrosion in HCl environment by 1-amino-2-mercapto-5-(4-(pyrrol-1-yl)phenyl)-1,3,4-triazole. S Afr J Chem Eng. 2022;39:42-51. doi: 10.1016/j.sajce.2021.11.009
11. Alamiery AA. Investigations on corrosion inhibitory effect of newly quinoline derivative on mild steel in HCl solution complemented with antibacterial studies. Biointerface Res Appl Chem. 2022; 12:1561-1568. doi: 10.33263/BRIAC122.15611568
12. Alkadir Aziz IA, Annon IA, Abdulkareem MH, Hanoon MM, Alkaabi MH, Shaker LM, Alamiery AA, Isahak WNRW, Takriff MS. Insights into corrosion inhibition behavior of a 5-mercapto-1, 2, 4-triazole derivative for mild steel in HCl solution: experimental and DFT studies. Lubricants. 2021; 9(9):122. doi: 10.3390/lubricants9120122
13. Aljibori HS, Alamiery A, Kadhum AAH, Advances in corrosion protection coatings: A comprehensive review. Int J Corros Scale Inhib. 2023;12:1476-1520.doi:10. 17675/2305-6894-2023-12-4-6.
14. Alamiery AA, Isahak WNRW, Takriff MS. Inhibition of mild steel corrosion by 4-benzyl-1-(4-oxo-4-phenylbutanoyl)thiosemicarbazide: Gravimetrical, adsorption and theoretical studies. Lubricants. 2021; 9(9):93. doi: 10.3390/lubricants9090093
15. Dawood MA, Alasady ZMK, Abdulazeez MS, Ahmed DS, Sulaiman GM, Kadhum AAH, Shaker LM, Alamiery AA. The corrosion inhibition effect of a pyridine derivative for low carbon steel in 1 M HCl medium: Complemented with antibacterial studies. Int J Corros Scale Inhib. 2021; 10:1766-1782. doi: 10.17675/2305-6894-2021-10-4-25
16. Alamiery AA. Corrosion inhibition effect of 2-N-phenylamino-5-(3-phenyl-3-oxo-1- propyl)-1,3,4-oxadiazole on mild steel in l M HCl medium: Insight from gravimetric and DFT investigations. Mater Sci Energy Technol. 2021; 4:398-406. doi: 10.1016/ j.mset.2021.09.002
17. Alamiery AA. Anticorrosion effect of thiosemicarbazide derivative on mild steel in 1 M HCl and 0.5 M sulfuric Acid: Gravimetrical and theoretical studies. Mater Sci Energy Technol. 2021; 4:263-273. doi: 10.1016/j.mset.2021.07.004
18. Alamiery AA, Isahak WNRW, Aljibori H, Al-Asadi H, Kadhum A. Effect of the structure, immersion time and temperature on the corrosion inhibition of 4-pyrrol-1-yln-(2,5-dimethyl-pyrrol-1-yl)benzoylamine in 1.0 M HCl solution. Int J Corros Scale Inhib. 2021; 10:700-713. doi: 10.17675/2305-6894-2021-10-2-14
19. Alamiery A, Mahmoudi E, Allami T. Corrosion inhibition of low-carbon steel in HCl environment using a Schiff base derived from pyrrole: gravimetric and computational studies. Int J Corros Scale Inhib. 2021; 10:749–765. doi: 10.17675/2305-6894-2021-10-2-17
20. Eltmimi AJM, Alamiery A, Allami AJ, Yusop RM, Kadhum AH, Allami T. Inhibitive effects of a novel efficient Schiff base on mild steel in HCl environment.

Int. J. Corros. Scale Inhib. 2021; 10:634-648. doi: 10.17675/2305- 6894-2021-10-2-10

21. Alamiery A, Shaker LM, Allami T, Kadhum AH, Takriff MS. A study of acidic corrosion behavior of furan-derived schiff base for mild steel in HCl environment: Experimental, and surface investigation. Mater Today: Proc. 2021; 44:2337–2341. doi: 10. 1016/j.matpr.2020.12.431
22. Al-Baghdadi S, Al-Amiery A, Gaaz T, Kadhum A. Terephthalohydrazide and isophthalohydrazide as new corrosion inhibitors for mild steel in HCl: Experimental and theoretical approaches. Koroze Ochr Mater 2021;65:12-22 . doi: 10.2478/kom-2021-0002
23. Hanoon MM, Resen AM, Shaker LM, Kadhum A, Al-Amiery A. Corrosion investigation of mild steel in aqueous HCl environment using n- (Naphthalen-1yl)-1-(4-pyridinyl)methanimine complemented with antibacterial studies. Biointerface Res Appl Chem. 2021;11:9735-9743.doi:10.33263/BRIAC112.97359743.
24. Al-Baghdadi S, Gaaz TS, Al-Adili A, Al-Amiery A, Takriff M. Experimental studies on corrosion inhibition performance of acetylthiophene thiosemicarbazone for mild steel in HCl complemented with DFT investigation. Int J Low-Carbon Technol. 2021; 16:181-188. doi: 10.1093/ ijlct/ctaa050
25. Al-Amiery A. Anti-corrosion performance of 2-isonicotinoyl-n-phenylhydrazinecarbothioamide for mild steel HCl solution: Insights from experimental measurements and quantum chemical calculations. Surf Rev Lett. 2021; 28:2050058. doi: 10.1142/ S0218625X20500584
26. Abdulazeez MS, Abdullahe ZS, Dawood MA, Handel ZK, Mahmood RI, Osamah S, et al. Corrosion inhibition of low carbon steel in HCl medium using a thiadiazole derivative: weight loss, DFT studies and antibacterial studies. Int J Corros Scale Inhib. 2021; 10:1812–1828. doi: 10.17675/2305-6894-2021-10-4-27
27. Mustafa A, Sayyid F, Betti N, Hanoon M, Al-Amiery A, Kadhum A, et al. Inhibition evaluation of 5-(4-(1H-pyrrol-1-yl)phenyl)-2-mercapto-1,3,4-oxadiazole for the corrosion of mild steel in an acid environment: thermodynamic and DFT aspects. Tribologia. 2021; 38:39-47. doi: 10.30678/fjt.105330
28. Abdulsahib YM, Eltmimi AJM, Alhabeeb SA, Hanoon MM, Al-Amiery AA, Allami T, et al. Experimental and theoretical investigations on the inhibition efficiency of N-(2,4-dihydroxytoluen-eylidene)-4-methylpyridin-2-amine for the corrosion of mild steel in HCl. Int J Corros Scale Inhib. 2021; 10:885-899. doi: 10. 17675/2305-6894-2021-10-3-3
29. Khudhair AK, Mustafa AM, Hanoon MM, Al-Amiery A, Shaker LM, Gazz T, et al. Experimental and theoretical investigation on the corrosion inhibitor potential of N-MEH for mild steel in HCl. Prog Color Colorant Coat. 2022; 15:111-122. doi: 10.30509/ PCCC.2021.166815.1111
30. Zinad DS, Salim RD, Betti N, Shaker LM, Al-Amiery AA. Comparative investigations of the corrosion inhibition efficiency of a 1-phenyl-2-(1-phenyl-ethylidene)hydrazine and its analog against mild steel corrosion in HCl solution. Prog Color Colorant Coat. 2022; 15:53-63. doi: 10.30509/ pccc.2021. 166786. 1108
31. Aljibori HS, Abdulzahra OH, Al Adily AJ, Al-Azzawi WK, Al-Amiery AA and Kadhum AAH, Recent progresses in thiadiazole derivatives as corrosion inhibitors in hydrochloric acid solution, Int J Corros Scale Inhib. 2023; 12(3):842-866. doi: 10.17675/2305-6894-2023-12-3-3
32. Rouin G, Abdelmouleh M, Mallah A, Masmoudi M. Oil extracted from spent coffee grounds as a green corrosion inhibitor for copper in a 3 wt. % NaCl solution. Coatings. 2023; 13(10):1745. https://doi.org/ 10.3390/coatings13101745.
33. Al-Sharabi HAA, Bouiti K, Bouhlal F, Labjar N. Anti-corrosive properties of Catha Edulis leaves extract on C38 steel in 1 M HCl media. Experimental and theoretical study. Inter J Corr Scale Inh. 2022; 11(3):956-984. doi:10.17675/2305-6894-2022-11-3-4
34. Bouhlal F, Mazkour A, Labjar H, Benmessaoud M, Serghini-Idrissi M, El Mahia M, Lotfi El M. El Hajjaji S, Labjar N. Combination effect of hydro-alcoholic extract of spent coffee grounds (HECG) and potassium Iodide (KI) on the C38 steel corrosion inhibition in 1 M HCl medium: Experimental design by response surface methodology. Chem Data Collect. 2020; 29: 100499. doi: 10.1016/j.cdc.2020.100499
35. Dehghani A, Bahlakeh G, Ramezanzadeh B, Ramezanzadeh M. Potential of borage flower aqueous extract as an environmentally sustainable corrosion inhibitor for acid corrosion of mild steel: Electrochemical and theoretical studies. J Mol Liq. 2019; 277: 895-911. doi: 10.1016/j.molliq. 2019.01.008
36. Kang J, Wen J, Jayaram SH, Yu A, Wang X, Development of an equivalent circuit model for electrochemical double layer capacitors (EDLCs) with distinct electrolytes, Electrohim Acta. 2014; 115: 587-598. doi: 10.1016/j.electacta.2013.11.002
37. Muñoz AI, Antón J, Guiñón JL and Herranz VP, Inhibition effect of chromate on the passivation and pitting corrosion of a duplex stainless steel in LiBr solutions using electrochemical techniques. Corros Sci. 2007; 49:3200-3225. doi: 10.1016/j.corsci. 2007.03.002
38. Yea Y, Yang D, Chen H, Guo S, Yang Q, Chen L, Zhao H and Wangb L, A high-efficiency corrosion inhibitor of N-doped citric acid-based carbon dots for mild steel in hydrochloric acid environment. J Hazard Mater. 2020;381:121019. doi:10.1016/j.jhazmat. 2019. 121019
39. Salim RD, Betti N, Hanoon M, Al-Amiery AA. 2-(2,4-Dimethoxybenzylidene)-N-phenylhydrazinecarbothio-amide as an efficient corrosion inhibitor for mild steel in acidic environment. Prog Color Colorant Coat. 2021; 15:45-52. doi: 10.30509/pccc.2021.166775.1105
40. ASTM International. Standard Practice for Preparing, Cleaning, and Evaluating Corrosion Test. ASTM International, 2011.

41. NACE International. Laboratory Corrosion Testing of Metals in Static Chemical Cleaning Solutions at Temperatures below 93°C (200°F), TM0193-2016-SG, 2000.
42. Frisch MJ, Trucks GW, Schlegel HB, Scuseria GE, Robb MA, Cheeseman JR, et al. Gaussian 03, Revision B. 05, Gaussian, Inc., Wallingford, CT, 2004.
43. Koopmans T. Ordering of wave functions and eigen-energies to the individual electrons of an atom. Physica. 1934; 1:104-113.
44. Al-Amiery AA, Shaker LM, Kadhum AH, Takriff MS. Exploration of furan derivative for application as corrosion inhibitor for mild steel in HCl solution: Effect of immersion time and temperature on efficiency. Mater Today: Proc. 2021; 42:2968-2973. doi: 10.1016/j.matpr.2020.12.807
45. Resen AM, Hanoon MM, Shaker LM, Kadhum A, Al-Amiery A. Exploration of 8-piperazine-1-ylmethylumbelliferone for application as a corrosion inhibitor for mild steel in HCl solution. Int J Corros Scale Inhib. 2021; 10:368-387. doi: 10.17675/2305-6894-2021-10-1-21
46. Hanoon MM, Resen AM, Al-Amiery A, Kadhum AH, Takriff MS. Theoretical and experimental studies on the corrosion inhibition potentials of 2-((6-methyl-2-ketoquinolin-3-yl)methylene)hydrazinecarbothioamide for mild steel in 1 M HCl. Prog Color Colorant Coat. 2021; 15(1):11-23. doi:10.30509/PCCC.2020. 166739. 1095
47. Hashim FG, Salman TA, Al-Baghdadi SB, Gaaz T, Al-Amiery AA. Inhibition effect of hydrazine-derived coumarin on a mild steel surface in HCl. Tribologia. 2020; 37:45-53. doi: 10.30678/fjt.95510
48. Resen AM, Hanoon MM, Salim RD, Al-Amiery AA, Shaker LM, Kadhum AA. Gravimetrical, theoretical, and surface morphological investigations of corrosion inhibition effect of 4-(benzoimidazole-2-yl)pyridine on mild steel in HCl. Koroze Ochr Mater. 2020; 64:122-130. doi: 10.2478/kom-2020- 0018
49. Salman AZ, Jawad QA, Ridah KS, Shaker LM, Al-Amiery AA. Selected BIS thiadiazole: synthesis and corrosion inhibition studies on mild steel in HCl environment. Surf Rev Lett. 2020; 27:2050014. doi: 10.1142/S0218625X20500146
50. Junaedi S, Al-Amiery A, Kadihum A, Kadhum A, Mohamad A. Inhibition effects of a synthesized novel 4-aminoantipyrine derivative on the corrosion of mild steel in HCl solution together with quantum chemical studies. Int J Mol Sci 2013; 14:11915-11928. doi: 10.3390/ijms140611915
51. Annon IA, Abbas AS, Al-Azzawi WK, Hanoon MM, Alamiery AA, Isahak WNRW and Kadhum AAH, Corrosion inhibition of mild steel in hydrochloric acid environment using thiadiazole derivative: Weight loss, thermodynamics, adsorption and computational investigations, S. Afr J Chem Eng. 2022; 41: 244-252. doi: 10.1016/j.sajce.2022.06.011
52. Al-Baghdadi S, Hashim F, Salam A, Abed T, Gaaz T, Al-Amiery A, et al. Synthesis and corrosion inhibition application of NATN on mild steel surface in acidic media complemented with DFT studies. Results Phys. 2018; 8:1178-1184. doi: 10.1016/j.rinp.2018.02.007
53. Al-Azzawi WK, Al Adily AJ, Sayyid FF, Al-Azzawi RK, Kzar MH, Jawoosh HN, et al. Evaluation of corrosion inhibition characteristics of an N-propionanilide derivative for mild steel in 1 M HCl: gravimetrical and computational studies. Int J Corros Scale Inhib. 2022; 11:1100-1114. doi: 10.17675/2305-6894-2022-11-3-12
54. Al-Amiery AA, Isahak WNRW, Al-Azzawi WK. Corrosion inhibitors: natural and synthetic organic inhibitors. Lubricants. 2023; 11:174. doi:10.3390/ lubricants11040174
55. Betti N, Al-Amiery AA, Al-Azzawi WK, Isahak WNRW. Corrosion inhibition properties of Schiff base derivative against mild steel in HCl environment complemented with DFT investigations. Scientific Reports. 2023; 13:8979. doi: 10.1038/s41598-023-36064-w
56. Al-Amiery A, Isahak WNRW, Al-Azzawi WK. ODHI: A promising isatin-based corrosion inhibitor for mild steel in HCl. J Mol Struct. 2023; 1288: 135829.https://doi.org/10.1016/j.molstruc.2023.135829.
57. Al-Amiery AA, Betti N, Isahak WNRW, Al-Azzawi WK, Wan Nik WMN. Exploring the effectiveness of isatin–schiff base as an environmentally friendly corrosion inhibitor for mild steel in HCl. Lubricants. 2023; 11:211. doi:10.3390/lubricants11050211
58. Al-Edan AK, Isahak WNRW, Che Ramli ZA, Al-Azzawi WK, Kadhum AAH, Jabbar HS, et al. Palmitic acid-based amide as a corrosion inhibitor for mild steel in 1M HCl. Heliyon. 2023; 9:e08625. doi: 10.1016/j.heliyon.2023.e14657
59. Naseef Jasim A, Abdulhussein BA, Mohammed Noori Ahmed S, Al-Azzawi WK, Hanoon MM, Abbass MK, Al-Amiery AA. Schiff's base performance in preventing corrosion on mild steel in acidic conditions. Prog Color Colorants Coat. 2023; 16(4):319-29. doi: 10.30509/pccc.2023.167081.1197
60. Mohammed A, Rubaye AY, Al-Azzawi WK, Alamiery A. Investigation of the corrosion inhibition properties of 4-cyclohexyl-3-thiosemicarbazide on mild steel in 1 M HCl solution. Prog Color Colorants Coat. 2023;16(4):347-59. doi: 10.30509/ PCCC. 2023. 167126.1212
61. Hussein SS, Al-Hasani IDD, Abed AM, Hanoon MM, Shaker LM, Al-Amiery A, et al. Antibacterial corrosion inhibitor for the protection of mild steel in 1 M HCl solution. Prog Color Colorant Coat. 2023; 16:59-70. doi: 10.30509/pccc.2022.166935.1149
62. Raheef KM, Qasim HS, Radhi AA, Al-Azzawi WK, Hanoon MM, Al-Amiery AA. Gravimetric and density functional theory investigations on 4-aminoantipyrin schiff base as an inhibitor for mild steel in HCl solution. Prog Color Colorant Coat. 2023; 16:255-269. doi: 10.30509/PCCC.2023.167077.1196
63. Alamiery A. Case study in a conceptual DFT investigation of new corrosion inhibitor. Lett Appl

Nano BioSci. 2021; 11:4007-4015. doi: 10.33263/ LIANBS114.40074015
64. Alamiery A. Effect of temperature on the corrosion inhibition of 4-ethyl-1-(4-oxo-4-phenylbutanoyl) thiosemicarbazide on mild steel in HCl solution. Lett Appl Nano BioSci. 2022; 11:3502-3508. doi:10. 33263/LIANBS112.35023508
65. Betti N, Al-Azzawi WK, Alamiery A. Synthesis and study of corrosion behavior of terephthalaldehyde-derived schiff base for low-carbon steel in HCl: experimental, morphological and theoretical investigation. KOM–Corr Mater Prot J. 2022; 66:103-112.
66. Carranza MS, Reyes YI, Gonzales EC, Arcon DP, Franco FC. Electrochemical and quantum mechanical investigation of various small molecule organic compounds as corrosion inhibitors in mild steel. Heliyon. 2021; 7(9):e07952. https://doi.org/ 10.1016/ j.heliyon.2021.e07952.
67. Khadom AA, Mahmmod AA. Quantum chemical and mathematical statistical calculations of phenyltetrazole derivatives as corrosion inhibitors for mild steel in acidic solution: a theoretical approach. Res Eng. 2022; 16:100741.https://doi.org/10.1016/j.rineng.2022.10074 1.
68. Malinowski S, Wróbel M, Woszuk A. Quantum chemical analysis of the corrosion inhibition potential by aliphatic amines. Materials. 2021; 14(20):6197.
69. Boulechfar C, Ferkous H, Delimi A, Berredjem M, Kahlouche A, Madaci A, Djellali S, Boufas S, Djedouani A, Errachid A, Khan AA. Corrosion inhibition of Schiff base and their metal complexes with [Mn (II), Co (II) and Zn (II)]: Experimental and quantum chemical studies. J Mol Liq. 2023; 378:121637.
70. Punitha N, Sundaram RG, Vengatesh G, Rengasamy R, Elangovan J. Bis-1, 2, 3-triazole derivative as an efficient corrosion inhibitor for mild steel in hydrochloric acid environment: Insights from experimental and computational analysis. Inorg Chem Commun. 2023; 153:110732.
71. Betti N and Al-Amiery A, Corrosion inhibition screening of 2-((6-aminopyridin-2-yl)imino)indolin-3-one: weight loss, morphology, and DFT investigations. Corros Sci Tech. 2023; 22(1): 10-20. doi: 10.14773/CST.2023.22.1.10.
72. Mahdi BS, Abbass MK, Mohsin MK, Al-Azzawi WK, Hanoon MM, AlKaabi MHH, Shaker LM, Al-Amiery AA, Isahak WNRW, Kadhum AAH, Takriff MS. Corrosion inhibition of mild steel in hydrochloric acid environment using terephthaldehyde based on Schiff base: Gravimetric, thermodynamic, and computational studies. Molecules. 2022; 27(15):4857. doi: 10.3390/molecules27154857 142.
73. Jawad QA, Zinad DS, Salim RD, Al-Amiery AA, Gaaz TS, Takriff MS, Kadhum AAH. Synthesis, characterization, and corrosion inhibition potential of novel thiosemicarbazone on mild steel in sulfuric acid environment. Coatings. 2019; 9(11):729. doi: 10.3390/coatings9110729.
74. Abbas AS, Mahdi BS, Abbas HH, Sayyid FF, Mustafa AM, Annon IA, Abdulsahib YM, Resen AM, Hanoon MM, Obaeed NH. Corrosion behavior optimization by nanocoating layer for low carbon steel in acid and salt media. Corros Sci Tech. 2023; 22(1):1-9. doi:10.14773/cst.2023.22.1.1
75. Sayyid FF, Mustafa AM, Hanoon MM, Saker LM, Alamiery AA. Corrosion protection effectiveness and adsorption performance of schiff base-quinazoline on mild steel in HCl environment. Corros Sci Technol. 2022; 21(4): 77-88. doi: 10.14773/CST.2022.21.2.77
76. Al-Amiery A, Shaker LM, Kadhum AAH and Takriff MS. Synthesis, characterization and gravimetric studies of novel triazole-based compound. Int J Low Carbon Technol. 2020;15(2):164-170. doi: 10.1093/ijlct/ctz067.
77. Mustafa AM, Abdullahe ZS, Sayyid FF, Hanoon MM, Al-Amiery AA, Isahak WN. 3-Nitrobenzaldehyde-4-phenylthiosemicarbazone as active corrosion inhibitor for mild steel in a hydrochloric acid environment. Prog Color Colorant Coat. 2022; 15(4):285-93. doi: 10.30509/PCCC. 2021.166869.1127
78. Abbass MK, Raheef KM, Aziz IA, Hanoon MM, Mustafa AM, Al-Azzawi WK, Al-Amiery AA, Kadhum AAH, Evaluation of 2-Dimethylamino-propionamidoantipyrine as a corrosion inhibitor for mild steel in HCl solution: A combined experimental and theoretical study. Prog Color Colorant Coat. 2024; 17: 1-10. doi: 10.30509/pccc.2023.167081.1197
79. Shanmugapriya R, Ravi M, Ravi S, Ramasamy M, Maruthapillai A. Electrochemical and morphological investigations of elettaria cardamomum pod extract as a green corrosion inhibitor for Mild steel corrosion in 1 N HCl. Inorg Chem Commun. 2023; 154:110958. doi: 10.1016/j.inoche.2023.110958
80. Al-Amiery AA, Al-Azzawi WK. Organic synthesized inhibitors for corrosion protection of carbon steel: A comprehensive review. J Bio Tribo Corros. 2023; 9(4):74. doi: 10.1007/s40735-023-00791-4

How to cite this article:
Resen AM, Jasim AN, Qasim HS, Hanoon MM, Al-Amiery AA, Waleed Khalid Al-Azzawi5, Ali M. Mustafa1, Firas F. Sayyid. Investigating the Corrosion Inhibition Performance of Methyl 3H-2,3,5-triazole-1-formate for Mild Steel in Hydrochloric Acid Solution: Experimental and Theoretical Insights. Prog Color Colorants Coat. 2024;17(2):185-205. https://doi.org/10.30509/ pccc.2023.167189. 1245.